

C. COMASCHI¹
G. VECCHI²
A.M. MALVEZZI¹
M. PATRINI² ✉
G. GUIZZETTI²
M. LISCIDINI²
L.C. ANDREANI¹
D. PEYRADE³
Y. CHEN^{3,4}

Enhanced third harmonic reflection and diffraction in Silicon on Insulator photonic waveguides

¹Dipartimento di Elettronica, Università degli Studi di Pavia, Via A. Ferrata 1, 27100 Pavia, Italy

²Dipartimento di Fisica “A. Volta”, Università degli Studi di Pavia, Via A. Bassi 6, 27100 Pavia, Italy

³Laboratoire de Photonique et de Nanostructures, CNRS, Route de Nozay, 91460 Marcoussis, France

⁴Département de Chimie, Ecole Normale Supérieure, 24 rue Lhomond, 75231 Paris Cedex 05, France

Received: 2 February 2005

Published online: 15 July 2005 • © Springer-Verlag 2005

ABSTRACT Enhanced third harmonic (TH) generation from Silicon-On-Insulator (SOI) planar waveguides as well as SOI photonic crystal (PhC) slabs is studied in different angular configurations, both in the visible and infrared energy ranges. In the SOI planar waveguide, the multilayer structure causes the optical properties such as TH reflection to be different from those of bulk silicon samples. This behavior is well reproduced by calculations of TH reflectance.

Measurements of third-harmonic reflection and diffraction from one-dimensional PhC slabs etched in the SOI waveguide are also reported. The angular positions of TH peaks at various diffraction orders agree well with those calculated from a nonlinear grating equation. Both reflection and diffraction processes contribute to enhanced TH generation efficiency in the PhC slabs.

TH reflectance measurements performed on PhC slabs in the near infrared show a resonant interaction between the incident beam and the photonic structure, dependent on the angle of incidence. This leads to a nonlinear conversion efficiency which is strongly enhanced with respect to that of the SOI waveguide, due to the excitation of strong local fields associated with the presence of photonic modes in the PhC slab.

PACS 42.70.Qs; 42.65.Ky

1 Introduction

The ability of guiding and localizing electromagnetic radiation in transparent media is becoming of paramount importance in telecommunication technology. Photonic crystals (PhCs) [1] seem to offer specific advantages in this respect in terms of flexibility in design and fabrication. The possibility of exploiting nonlinear effects in PhCs, which can be enhanced with *ad hoc* design of photonic mode dispersion, opens up further options. Theoretical studies have already predicted enormous gain factors of harmonic generation in

carefully designed photonic structures [2]. Nonlinear second- and third-harmonic generation have also been observed and studied in Si multilayers [3], GaAs [4, 5], GaN [6, 7] PhC waveguides, and opals [8].

Among these various candidates, silicon-based optical devices hold promise of complete integration with microelectronics circuitry. In particular, Silicon-On-Insulator (SOI) waveguide technology is emerging as a suitable platform for integrated photonic circuits. An advantage of SOI planar waveguides is the large contrast in refractive-index displayed between silicon and silica (insulator) layers, which allows photon confinement in small waveguides and along sharp bends [9]. In SOI PhC slabs, only a thin silicon core layer needs to be patterned, leading to photonic structures with high optical quality.

In this paper we present and discuss several experimental results of third harmonic generation (THG) from SOI planar waveguides, both in the bare configuration and etched in the form of one-dimensional (1D) PhC slabs. The generation of coherent harmonic radiation is studied by exploring different angular configurations, with a pump wavelength around 800 nm as well as in the infrared (around 1.5 μm) range. Third-harmonic (TH) reflection and diffraction in the 1D photonic crystals are discussed. In particular, we report the first observation of resonant enhancement of THG in SOI PhC slabs when the pump beam is frequency- and momentum- matched to a photonic mode of the structure. The results are compared with a theory of the nonlinear conversion process, which takes into account the local-field effects related to the formation of photonic modes in the patterned slab structure.

2 Samples and experiment

The waveguides investigated here are SOI wafers produced by SOITEC by the use of the so-called Smart CutTM process [10]. The SOI vertical structure is made of a silicon substrate, a SiO₂ layer, and a thin silicon top layer. The very unequal refractive indexes of silica ($n \sim 1.45$) and silicon ($n \sim 3.5$) define a planar waveguide, whose silica cladding and silicon core layers are 1 μm and 0.26 μm thick, respectively.

✉ Fax: +39-0382-987-563, E-mail: patrini@fisicavolta.unipv.it

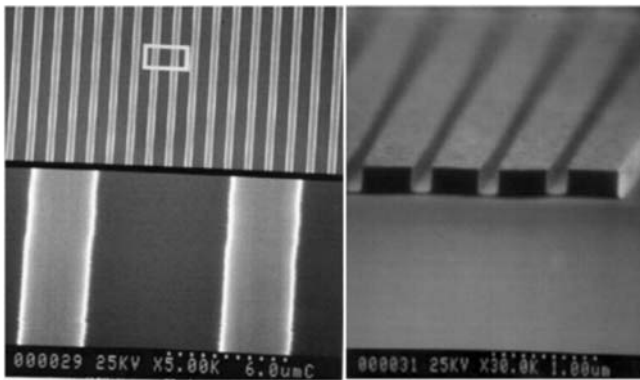


FIGURE 1 SEM image of L3 sample (left, top view) and of L4 sample (right, side view)

The photonic crystal waveguides have been fabricated by applying standard electron-beam lithography and reactive-ion etching techniques [11]. In the present work we examine the bare waveguide system and two different 1D lattices of silicon stripes. One sample, named L3, is defined by a lattice constant $a = 1 \mu\text{m}$ and an air filling factor $f = 0.7$, while the second one, named L4, by $a = 0.65 \mu\text{m}$ and $f = 0.18$, respectively. Two Scanning Electron Microscope (SEM) images of the samples are reported in Fig. 1, showing the high quality of the fabricated structures. We remark that the grooves have been aligned along the [110] direction of silicon. Variable-angle reflectance measurements on these samples, which led to the photonic band structure for the two polarizations were previously reported [12].

The geometry of the experimental layout is sketched in Fig. 2, including notations for the angles involved in the experiment. They are the angle of incidence θ of the pump radiation, the angle ϕ formed by the Γ -X lattice direction to the plane of incidence, and the polar diffraction angle θ' measured from normal \mathbf{n} to the sample. Only in-plane diffraction

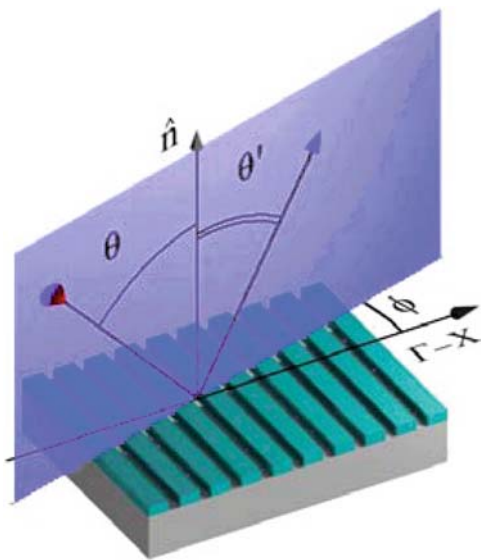


FIGURE 2 Geometry of the optical setup for TH nonlinear measurements. The excitation laser beam impinges from the left. The in-plane angle θ' identifies the direction of radiation collection by an optical fiber

beams (forward and backwards) are detected. All measurements, except for azimuthal ones, are performed along the Γ -X direction, i.e., for radiation incident perpendicular to the grooves of the PhCs.

Crystalline silicon exhibits a very low second harmonic generation, since inversion symmetry in a centrosymmetric medium forbids an electrical-dipole bulk second-order susceptibility ($\chi^{(2)}$) [13]. Actually, SHG in crystalline silicon is due to dipolar-surface, dipolar-interface and quadrupolar-bulk terms.

On the other hand, the THG process does not require the lack of inversion symmetry and is quite efficient in silicon. The harmonic generation process is utilized here for investigating photonic structures by means of nonlinear spectroscopy and for exploiting resonant conditions between e.m. field and PhCs to maximize nonlinear effects.

Two laser sources are used for experiments, a Ti:sapphire laser and an optical parametric oscillator (OPO), both providing pulses of about 130 fs in duration, with 80 MHz repetition rate, emitting around 800 nm and 1400–1660 nm, respectively. Pulses are focused down to spots 30–50 μm in diameter onto the sample, after traveling across color filters and an intensity control system. The radiation at TH frequency, which is generated in reflection and diffraction from the sample surface, is collected by an optical fiber (1 or 0.4 mm core diameter) into a cooled photomultiplier (PMT). A suitable combination of color and interference filters is used to reject the pump radiation. The detection of the TH signal is performed using a light chopper to modulate the pump radiation. The PMT signal is then recorded by an averaging oscilloscope so that the amplitude of the signal with respect to background is evaluated. Nonlinear reflection (and diffraction) in third harmonic has been evaluated in all experiments in terms of pulse intensities I as $R_{\text{nl}} = I(3\omega)/I^3(\omega)$, reported in arbitrary units, *albeit* consistent in each set of measurements.

3 The SOI planar waveguide

Intense third harmonic signals at 270 nm are observed when SOI planar waveguides are illuminated with 810 nm laser pulses. The characteristic cubic dependence is well verified and illustrated in Fig. 3.

As reported later on, the unpatterned waveguide has been chosen to represent the standard specimen, for comparison with the optical response from 1D patterned samples. The SOI waveguide is a composite structure compared to bulk silicon, and this fact is particularly well evidenced when the nonlinear optical characterization is involved. In Fig. 4 THG in reflection from the slab top surface and from a sample of crystalline silicon for both p - and s -polarizations has been investigated by rotating the samples around their normal direction. The well-known [14–16] anisotropic behavior of THG in reflection from (001)-orientation of crystalline silicon is observed, showing a fourfold dependence on the azimuthal angle. This behavior originates from the microscopic tensorial symmetry of nonlinear susceptibility. Moreover, the SOI third harmonic reflectance is more intense than the bulk Si counterpart by two orders of magnitude.

Measurements in Fig. 4 were performed at 45° of incidence, but this enhancement between the two systems is

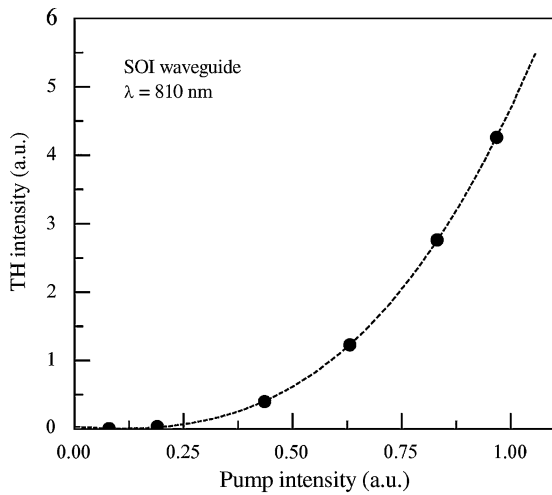


FIGURE 3 Third harmonic intensity generated in reflection from a SOI waveguide as a function of pump intensity at 810 nm. The dotted line is a cubic best fitting of the data

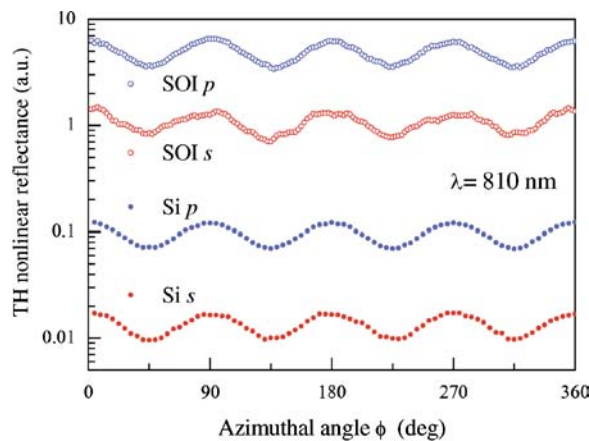


FIGURE 4 Experimental TH nonlinear reflectivity as a function of azimuthal angle from the surface of the SOI planar waveguide (open circles) and of (100) bulk silicon sample (full circles), for p -polarized pump (blue) and s -polarized pump (red). The parameters are $\lambda = 810$ nm and $\theta = 45^\circ$

generally present also for most angles of incidence. Indeed, the vertical four-layer stacking of SOI, considering the silicon substrate, too, causes the optical properties such as TH reflection to be amplified. In our case, multiple reflections of the pump beam from interfaces result in constructive interference of fundamental field into the core Si layer.

The waveguiding configuration strongly modifies also the TH nonlinear reflectance when measured *versus* the angle of incidence θ , as indicated in Figs. 5 and 6. This angular trend is completely different from the corresponding bulk silicon response [14]. In particular, Fig. 5a and b shows TH nonlinear reflectance measured for s - (p -) input polarization, at 810 nm of pump wavelength. The TH reflectance calculations are also displayed in the figures. They have been performed with the method of nonlinear transfer matrix [17], which takes full account of interference in the multilayer SOI structure, as well as absorption at the harmonic frequency through the imaginary part of the complex refractive index. In both cases, the displayed agreement between measured and calculated data is quite satisfactory.

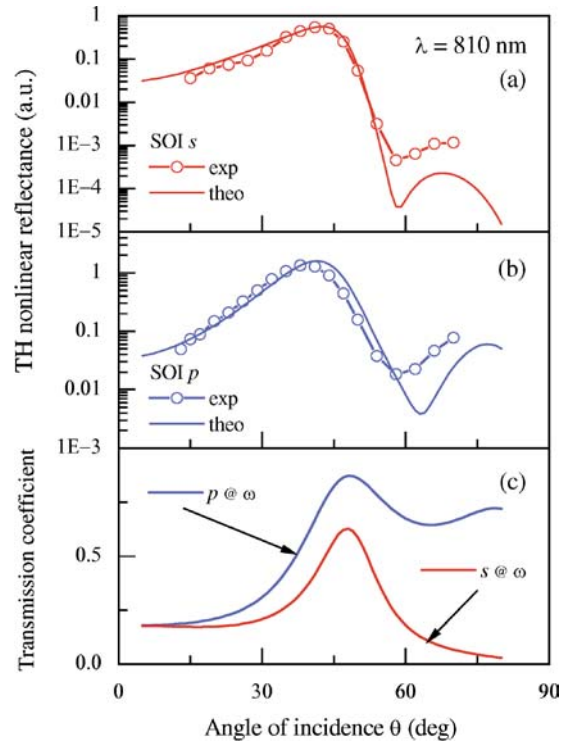


FIGURE 5 Experimental (open circles) and calculated (continuous lines) TH nonlinear reflectance at 810 nm as a function of the angle of incidence, of SOI planar waveguide, for **a** s and **b** p input polarizations. Panel **c**: calculated linear transmission coefficients at ω for the two polarizations indicated

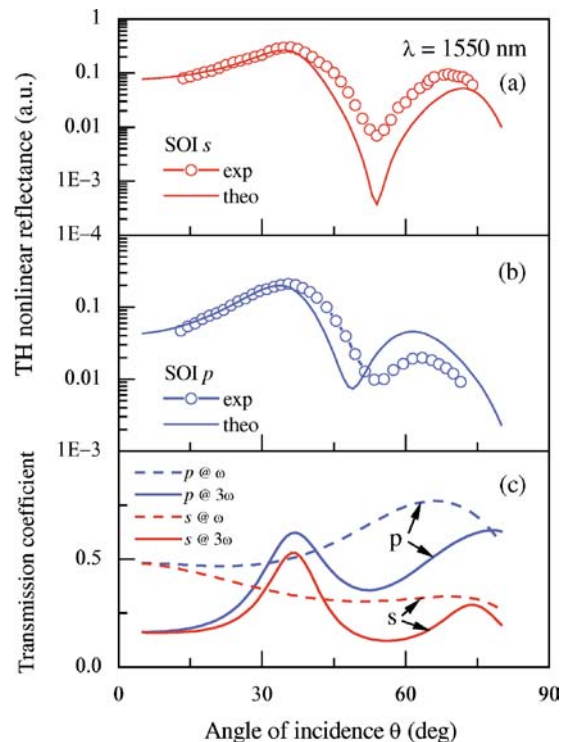


FIGURE 6 Experimental (open circles) and calculated (continuous lines) TH reflectance at 1550 nm as a function of the angle of incidence, of SOI planar waveguide, for **a** s and **b** p input polarizations. Panel **c**: calculated linear transmission coefficients at ω (solid lines) and 3ω (dashed lines) for the two polarizations indicated

In Fig. 5, besides a minimum of third harmonic signal common to both polarizations and appearing around 60° , two maxima are detected, the one at smaller angle of incidence being more pronounced. Notice that more than two orders of magnitude in the TH intensity modulation are measured. Figure 6 refers to the same measurements taken at 1550 nm. Again a strong modulation of the nonlinear reflectance is observed as a function of the angle of incidence. Two major differences are, however, apparent. A shift of the whole curve (minima and maxima) is observed together with a shallower modulation depth. In Figs. 5 and 6, panel (c), the linear Fresnel transmission coefficients calculated for the multilayer structure are plotted. In the first case, for $\lambda = 810$ nm, the TH escape length is less than 10 nm (the TH linear transmission coefficient across the waveguide is zero for both polarizations), while the pump beam is fully propagating across the multilayer. We observe that the angular behavior of TH reflectance originates from the linear transmission at ω .

When the pump wavelength is $\lambda = 1550$ nm, the TH beams propagate along the structure (the penetration depth is about 1.4 micron) and the pump beam is not affected by absorption. In this case the nonlinear SOI reflectance is heavily affected by the response of the system at the TH frequency. The TH reflectance closely follows the angular behavior of the linear transmission coefficient at 3ω , thus reflecting the higher extraction efficiency of the TH field generated in the silicon waveguide.

Concluding this section, TH reflectance in the SOI waveguide is higher than in bulk silicon due to the vertical confinement effect in the slab. The wavelength and angular dependence of TH generation is quite complex due to an interplay of linear propagation at ω and 3ω and of absorption.

4 Nonlinear diffraction

The two 1D photonic crystals obtained from the SOI waveguide exhibit even stronger third order effects. As an example, Fig. 7 illustrates the diffraction pattern of both samples when illuminated at 810 nm with p -polarized radiation and at 54° of incidence. The bare SOI reflection pattern

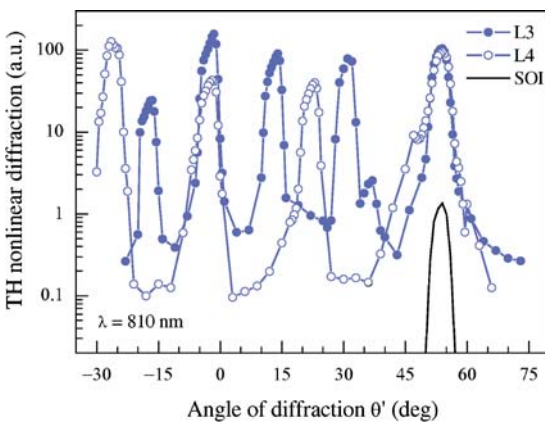


FIGURE 7 In-plane third harmonic ($\lambda = 270$ nm) diffraction pattern for samples L3 and L4 observed when pumping with p -polarized 810 nm pulses as a function of the angle of diffraction. The angle of incidence is 54° and the reflected TH signal from the bare SOI waveguide is shown

is also shown for comparison. Notice that the widths of the diffraction peaks appearing in Fig. 7 are mainly determined by the collection angle of the fiber used for detection, and are of the order of ± 1 degree.

The choice of the angle of incidence is motivated by the coincidence in zero-order diffraction intensities for both PhCs (see Fig. 10 below). In several experimental runs, the nonlinear Bragg condition for diffracted beams [18, 19],

$$\mathbf{k}'_{\parallel}(3\omega) = 3\mathbf{k}_{\parallel}(\omega) + \mathbf{G}, \quad (1)$$

has been verified for various angles of incidence.

In Eq. (1) $\mathbf{k}_{\parallel}(\omega)$ is the parallel component of incident wavevector, $\mathbf{k}'_{\parallel}(3\omega)$ is the diffracted in-plane component at third harmonic, and \mathbf{G} is a 1D reciprocal lattice vector. In terms of the incidence and diffraction angles, the equation becomes

$$\sin \theta' = \sin \theta + m \frac{\lambda}{3a}. \quad (2)$$

$m = 0$ simply defines THG in specular reflection. The plot of Eq. (2) is reported in Fig. 8, illustrating the angular positions of diffracted TH orders, at a pump wavelength $\lambda \sim 810$ nm and for L3 sample. Measured points agree well with calculated lines, confirming this general kinematic law. By exploring the plane of incidence with the collecting optical fiber, both positive and negative orders of diffraction in THG are observable. The diffraction peaks appear prominent over a low background of TH signal, as shown in Fig. 7.

Figure 9 illustrates the TH diffraction spots as they appear on a white paper screen and recorded by an ordinary camera. The blue color is here due to the paper fluorescence and can also be easily observed with the naked eye. The spatial coincidence of pump and TH beams results in the superposition of red and blue spots in the case of 0th and 3rd orders only ($m = 0$ and $m = -3$ in Eq.(2)). The TH diffraction has been verified in the short wavelength range to reach a high number of diffraction orders, due to the ratio $\lambda / 3a < 1$. On the contrary, when pumping sample L3 with $\lambda \sim 1500$ nm laser radiation only the first diffraction order exists in the plane.

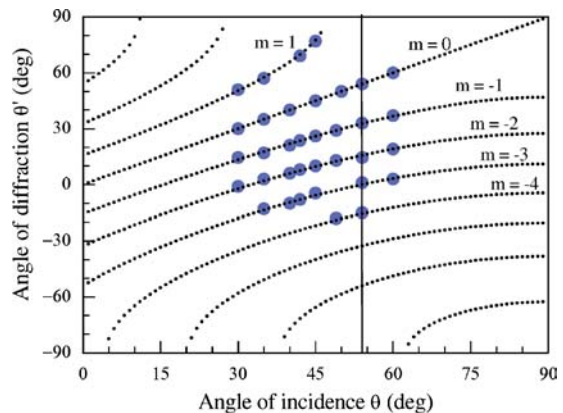


FIGURE 8 Plot of diffraction orders for TH at $\lambda = 270$ nm in the (θ, θ') plane. The reflected beams are also included. The filled circles are the measured angular positions, while the calculation is represented by dotted lines. The investigated photonic crystal is sample L3. The vertical line refers to the diffraction profiles illustrated in Fig. 7

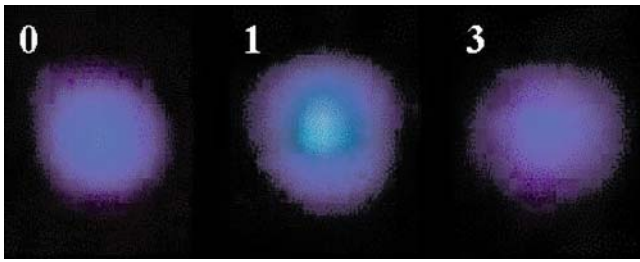


FIGURE 9 Photo images of three of the peaks reported in Fig. 7 corresponding to the zeroth, first and third orders of diffraction of sample L3. The spot corresponding to order 1 is blue-colored only, while the other two are the superposition of pump (red) and TH (blue) radiation beams

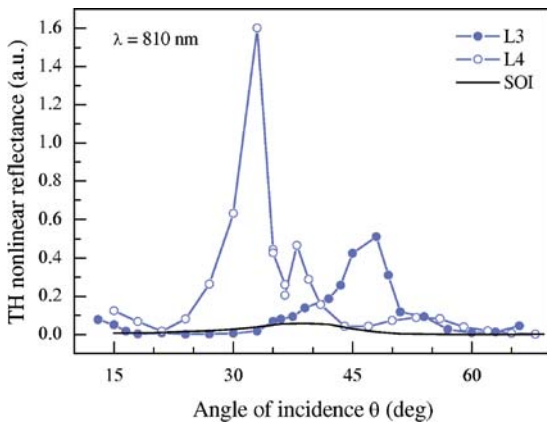


FIGURE 10 Measured TH reflectance as a function of the angle of incidence from the photonic crystal L4, (empty circles), L3 (filled circles) and the SOI waveguide (solid line). *p*-polarized pump radiation, at $\lambda = 810$ nm is incident perpendicular to the grooves

The intensities of diffracted TH beams turn out to be of the same order as that of reflected signal. For some diffraction orders, notably the 3rd order peaks of Fig. 7, they even exceed these values. In any case a comparison between reflected TH beams for our PhCs and the bare waveguide reveals a signal enhancement up to two orders of magnitude, as shown in Fig. 7. This value is further increased by a factor ≈ 4 when the overall TH emission on all spectral orders is considered.

In Fig. 10 we follow the TH reflectance ($m = 0$) as a function of the angle of incidence for all three samples. The trend associated to the unpatterned slab is similar to those shown in Fig. 5, with slight differences in maxima and minimum positions. In L3 and L4 samples the PhC structure produces analogous modulations which appear to be shifted in angular position by different amounts depending upon the photonic pattern and air filling fraction. Anyway, it is clear that the efficiency of TH generation in the 1D photonic crystal slabs is higher than in the unpatterned SOI waveguide: this follows from taking either the maxima, or the average of the curves shown in Fig. 10. The enhancement of TH generation in the patterned systems (even with a reduced fraction of nonlinear material) is attributed to the effect of field enhancement at the edges of the sidewalls, which leads to strong amplification of the nonlinear process.

5 Resonant coupling

We now turn to the search for resonant coupling of the laser radiation with photonic modes of the structure in the radiative region, i.e., above the light line of air. Several reasons motivate the selection of infrared wavelengths for this analysis. First, and most importantly, the effect of disorder grows like ω^4 (as appropriate for Rayleigh scattering) leading to large inhomogeneous linewidths for higher-lying bands. Photonic band calculations are increasingly less accurate at high energies, also because the present PhC slabs become multimode with several folded bands in the visible region [12]. This occurrence limits considerably the possibility of selecting correct resonant conditions in the experiment when pumping around $\lambda = 800$ nm. Finally, one expects that for lower lying bands confinement effects are stronger; therefore, higher fields may be obtained. In the following the discussion is limited to sample L4, since sample L3 exhibits very weak photonic structures in the spectral regions considered [12].

In Fig. 11 the nonlinear TH reflectance measured from the PhC slab at 1550 nm shows an intense peak around $\theta = 18^\circ$, which is more than 200 times the corresponding one from the bare slab at the same value of the incidence angle. For other choices of the fundamental wavelength, we have reported even higher increment factors [20]. At resonance, the reflected (and also the in-plane diffracted) TH beam is visible to the naked eye as a green spot. The amount of TH signal modulation due to the resonant coupling to photonic modes is orders of magnitude larger than that induced by interference effects in SOI vertical stacking.

We emphasize that the present experiments are conducted in a surface reflectance geometry, in which the incident electromagnetic wave does not propagate along the waveguide plane. Therefore the comparison between TH generation efficiencies of the SOI PhC and of the bare waveguide can be done without introducing a coherence length, which is not easily defined for a PhC slab. If the TH efficiencies in the two systems are compared by taking the maxima of the curves in Fig. 11 (instead of the values at the same angle $\theta = 18^\circ$), the resonant enhancement in the PhC with respect to the SOI waveguide is still found to be about two orders of magnitude.

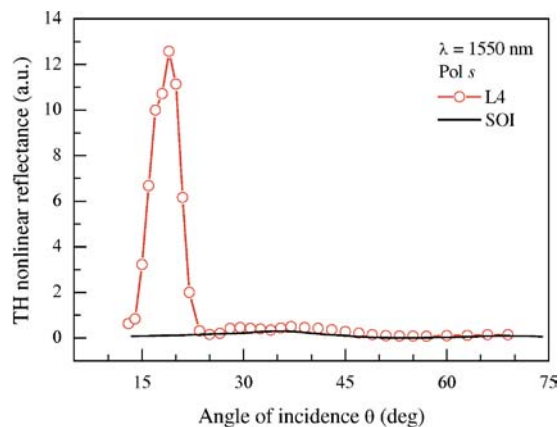


FIGURE 11 Measured TH nonlinear reflectance as a function of angle of incidence from the photonic crystal L4 (open circles) and from the SOI waveguide (continuous line). The *s*-polarized pump radiation is at $\lambda = 1550$ nm. The ratio between L4 and SOI maxima is ~ 200

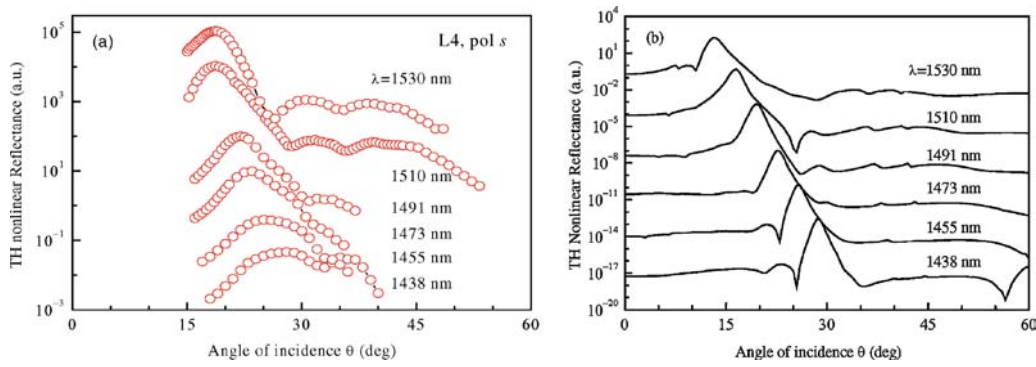


FIGURE 12 a, b Experimental (theoretical) behavior of third-harmonic nonlinear reflectance of sample L4, as a function of the angle of incidence for various wavelengths, with *s*-polarized pump. The curves are offset for clarity

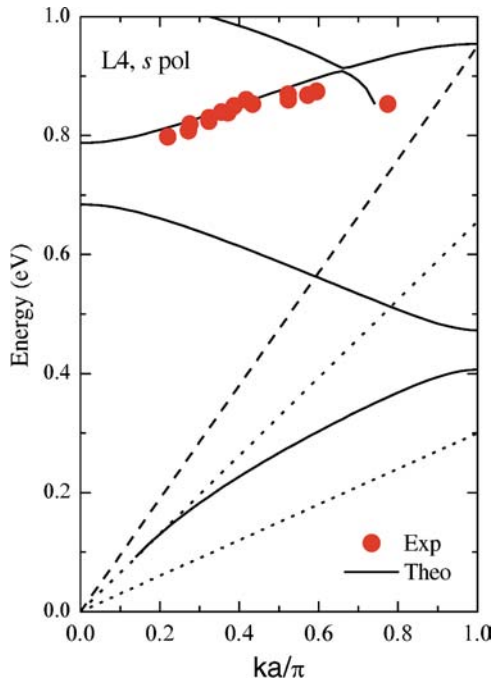


FIGURE 13 Photonic band dispersion for sample L4 obtained from peak positions of TH nonlinear reflectance (full circles). The calculated photonic bands are indicated with solid lines. The dashed line represents the light dispersion in air, while dotted lines refer to light dispersion in SiO₂ and in silicon

The physical origin of the resonant coupling is a frequency- and momentum-matching between the incident radiation and a photonic mode lying above the air light line. This effect, which strongly localizes the electric field and nonlinear polarization in the silicon layer, was theoretically predicted in [2] and previously reported in GaAs [4, 5] and GaN [6, 7] systems. The broadening of the resonant features observed in the present experiment is largely dependent on the bandwidth of 130 fs laser pulses. Spectral analysis should be necessary to finely resolve sharp photonic features and, eventually, to detect higher signal enhancement ratios.

The resonant peaks of TH signal illustrated in Fig. 12a (where the experimental curves are vertically displaced by a constant amount) move towards smaller angles of incidence with increasing pump wavelength. When compared to the cal-

culated angular plots in Fig. 12b, it appears that the observed resonance peaks as well as their angular shifts as a function of pump wavelength, are reproduced consistently. The calculation has been performed using a scattering matrix method [21], implemented with a nonlinear extension, which allows calculating the electric field and nonlinear polarization in real space.

The angular dispersion of TH peak reflects the $\omega(k)$ dispersion of a photonic mode, as shown in Fig. 13. The figure shows the band diagram of the L4 sample in the case of *s* (transverse electric) polarization [12]. The size of the experimental points is a measure of the error bars, which relates to the spectral width of pump pulses as well as to the acceptance angle of the detection system. This diagram demonstrates that the resonance with photonic modes is indeed responsible for the large enhancement of the TH signal in the 1D PhC slab as compared to the unpatterned waveguide sample.

6 Conclusions

In this work results on third harmonic generation in 1D SOI photonic crystals are presented and compared with those on bare configuration, i.e., the unpatterned SOI waveguide. The investigation has revealed an unexpected richness in the nonlinear effects encountered. The experiments have been conducted in two different frequency ranges for the excitation radiation, namely around 800 nm and 1.5 μm . TH reflectance, waveguide interference effects, and nonlinear Bragg diffraction have been observed and investigated in relation with the interplay of pump and TH beams propagation. Basically, the THG efficiency increases when going from bulk silicon to the SOI waveguide, due to vertical confinement in the slab, and when patterning the waveguide due to field enhancement at the sidewall edges.

The addition of a 1D photonic pattern to a SOI waveguide improves dramatically the nonlinear performances of the system when resonance effects are involved. Up to two orders of magnitude in TH reflectance are gained when the pump beam is resonant with a photonic mode of the structure. These results are in line with the aim of obtaining silicon-based nonlinear structures operating in the 1.5 micron window and suggest that quasi phase matched TH operation is feasible by a proper design of SOI-based devices.

ACKNOWLEDGEMENTS This work was supported by MIUR through FIRB project "Miniaturized electronic and photonic systems" as well as Cofin programs, and by EU Network of Excellence PHOREMOST.

REFERENCES

- 1 See Feature Issue, *Nonlinear Optics of Photonic Crystals*, ed. by C.M. Bowden, A.M. Zheltikov, J. Opt. Soc. Am. B **19**, 1961 (2002)
- 2 A.R. Cowan, J.F. Young, Phys. Rev. B **65**, 085106 (2002)
- 3 T.V. Dolgova, A.I. Mailykovski, M.G. Martemyanov, A.A. Fedyanin, O.A. Aktsipetrov, JETP Lett. **75**, 15 (2002); M.G. Martemyanov, E.M. Kim, T.V. Dolgova, A.A. Fedyanin, O.A. Aktsipetrov, G. Marowsky, Phys. Rev. B **70**, 073311 (2004)
- 4 A.M. Malvezzi, G. Vecchi, M. Patrini, G. Guizzetti, L.C. Andreani, F. Romanato, L. Businaro, E. Di Fabrizio, A. Passaseo, M. De Vittorio, Phys. Rev. B **68**, 161306 (R) (2003)
- 5 J.P. Mondia, H.M. van Driel, W. Jiang, A.R. Cowan, J.F. Young, Opt. Lett. **28**, 2500 (2003)
- 6 J. Torres, D. Coquillat, R. Legros, J.P. Lascaray, F. Teppe, D. Scalbert, D. Peyrade, Y. Chen, O. Briot, M. Le Vassor d'Yerville, E. Centeno, D. Cassagne, J.P. Albert, Phys. Rev. B **69**, 085105 (2004)
- 7 G. Vecchi, J. Torres, D. Coquillat, M. Le Vassor d'Yerville, A.M. Malvezzi, Appl. Phys. Lett. **84**, 1245 (2004)
- 8 P.P. Markowicz, H. Tiryaki, H. Pudavar, P.N. Prasad, N.N. Lepeshkin, R.W. Boyd, Phys. Rev. Lett. **92**, 083903 (2004)
- 9 K.K. Lee, D.R. Lim, H.-C. Luan, A. Agarwal, J. Foresi, L.C. Kimerling, Appl. Phys. Lett. **77**, 1617 (2000)
- 10 G.K. Celler, S. Cristoloveanu, J. Appl. Phys. **93**, 4955 (2003)
- 11 D. Peyrade, Y. Chen, A. Talneau, M. Patrini, M. Galli, F. Marabelli, M. Agio, L.C. Andreani, E. Silberstein, Ph. Lalanne, Microelectron. Engin. **61-62**, 529 (2002)
- 12 M. Patrini, M. Galli, F. Marabelli, M. Agio, L. C. Andreani, D. Peyrade, Y. Chen, IEEE J. Quantum Electron. **38**, 885 (2002)
- 13 Y.R. Shen, *The Principles of Nonlinear Optics*, (Wiley, New York 1984)
- 14 W.K. Burns, N. Bloembergen, Phys. Rev. B **4**, 3437 (1971)
- 15 C.C. Wang, J. Bomback, W.T. Donlon, C.R. Huo, J.V. James, Phys. Rev. Lett. **57**, 1647 (1986)
- 16 T. Tsang, Phys. Rev. A **52**, 4116 (1995)
- 17 D.S. Bethune, J. Opt. Soc. Am. B **6**, 910 (1989)
- 18 A.M. Malvezzi, F. Cattaneo, G. Vecchi, M. Falasconi, G. Guizzetti, L.C. Andreani, F. Romanato, L. Businaro, E. Di Fabrizio, A. Passaseo, M. De Vittorio, J. Opt. Soc. Am. B **19**, 2122 (2002)
- 19 I. Freund, Phys. Rev. Lett. **21**, 1404 (1968)
- 20 G. Vecchi, A.M. Malvezzi, M. Patrini, G. Guizzetti, L.C. Andreani, M. Liscidini, Y. Chen, D. Peyrade, SPIE Proc. **5450**, 260 (2004)
- 21 D.M. Whittaker, I.S. Culshaw, Phys. Rev. B **60**, 2610 (1999)